Available online at www.sciencedirect.com
ScienceDirect
Geochimica et Cosmochimica Acta 70 (2006) 4850–4861
Geochimica
www.elsevier.com/locate/gca

Time-dependent sorption of Cd^{2+} on CaX zeolite: Experimental observations and model predictions

Imad A.M. Ahmed, Scott D. Young *, Neil M.J. Crout

School of Biosciences, Division of Agriculture and Environmental Sciences, University of Nottingham, University Park, Nottingham, NG7 2RD, UK

Received 28 November 2005; accepted in revised form 14 July 2006

Abstract

Sorption, fixation and desorption kinetics of Cd^{2+} on calcium-exchanged zeolite-X were studied using an isotopic dilution technique utilizing ^{109}Cd. The technique provided reliable measurements of time-dependent fixation of Cd and was validated using chabazite, which demonstrated wholly reversible Cd^{2+} ion exchange. A first-order kinetic model was developed to describe the progressive transfer of Cd^{2+} to a less reactive form in X-zeolite, following initial sorption, and subsequent desorption of Cd subject to different initial contact times. The kinetic model differentiates between two 'pools' of sorbed Cd^{2+} on zeolite-X, designated labile and non-labile sorbed Cd in which the labile sorbed Cd is in immediate equilibrium with the free Cd^{2+} ion activity in solution. Additionally, an intra-particle diffusion model was developed and compared with the kinetic model to determine whether time-dependent Cd sorption is controlled by reaction kinetics or diffusion within zeolite particles. The kinetic model provided a much better fit to the experimental data ($R^2 = 0.987$) than the diffusion model. The rate constants describing Cd dynamics in CaX zeolite gave a half-time for Cd desorption of ~77 d, for release to a 'zero-sink'.

1. Introduction

Zeolites are microporous crystalline aluminosilicates; their framework exhibits negative charge because of the isomorphous substitution of Al^{3+} for Si^{4+}. These negative charges appear on the AlO_4^- groups of the framework and are compensated by extra-framework cations or through the interaction of framework oxygen atoms and protons with the formation of acid hydroxyls (Breck, 1974; Dyer, 1988).

The application of synthetic zeolites (e.g., A-, X-, and Y-zeolite) to ameliorate environmental pollution, particularly in relation to the removal of trace metal cations from contaminated waters, has received extensive attention and has been reported previously (Nikashina et al., 1976; Nava et al., 1995; Biskup and Subotic, 1998; Keane, 1998; Biskup and Subotic, 2000; Garcia-Sosa and Solache-Rios, 2001; Kim and Keane, 2002; Barros et al., 2004; Shevade and Ford, 2004). Synthetic zeolites have been the subject of considerable scientific and industrial interest due to their large ion exchange capacity, thermal and hydrothermal stability, large internal surface area, and well-defined framework structures. In addition, and in contrast to natural zeolites, the phase purity of synthetic zeolites makes it easier to obtain reproducible and interpretable results in sorption experiments.

Previous investigations of zeolite chemistry have focused primarily on the selectivity and efficiency of the zeolitic material in removing heavy metals from solution. It is generally accepted that zeolites sorb metal cations through a single ion exchange mechanism that is fast and reversible (Helfferich, 1962; Breck, 1974; Colella, 1996). However, it has been reported that ion exchange of monovalent ions is faster than that of divalent ions in zeolites (Barrer et al., 1963; Barrer et al., 1969). In addition, some studies have reported that transition-metal ions may bind to

* Corresponding author. Fax: +44 0 115 951 3251.
E-mail address: Scott.Young@Nottingham.ac.uk (S.D. Young).

0016-7037/$ - see front matter © 2006 Elsevier Inc. All rights reserved.
doi:10.1016/j.gca.2006.07.011

X- and Y-zeolites irreversibly (Lai and Rees, 1976; Fletcher and Townsend, 1982). In view of these previous reports, further investigations of the reversibility of exchange of Ca^{2+}, Cd^{2+}, Zn^{2+}, Mn^{2+}, Co^{2+}, Ni^{2+}, and Cu^{2+} ions were performed by Fletcher and Townsend (1985). They attempted to elute all the metal ions out of zeolites and found that Ca^{2+} showed no capacity for irreversible binding whereas ~1% of Cd^{2+} in zeolite-X was irreversibly bound, compared with >20% Cu^{2+}, 10% Ni^{2+}, 5% Co^{2+}, 0.3% Mn^{2+}, and 0.5% Zn^{2+}. However, all these studies investigated metal irreversibility in faujasite systems following a short ion-exchange time. Thus, scant attention has been given to the effect of prolonged contact time (weeks or months) on trace metal ion sorption by zeolites, especially under conditions found in natural systems and permeable reactive barriers (PRBs) installed to protect groundwaters from metal pollution. Such kinetic studies would be useful to assess the risk of pollutant release, following initial sorption, and thereby indicate the long-term viability of remediation strategies such as PRB deployment. In the work reported here the effect of contact times up to 100 d on Cd^{2+} sorption by calcium-exchanged zeolite-X was studied using an isotopic dilution method utilizing ^{109}Cd as a tracer. In addition, the concentration of labile and non-labile Cd was quantified over time and the process of extended Cd^{2+} sorption was modeled using kinetic and diffusion models. Labile (sorbed) Cd can respond rapidly to any change in Cd^{2+} activity in the solution phase whereas non-labile Cd is unresponsive, possibly due to occlusion within solid matrices or perhaps due to the formation of kinetically restricted surface complexes. The main focus of this work was to examine the dynamics of Cd sorption and fixation on zeolite rather than determine the underlying mechanisms.

2. Materials and methods

2.1. Materials

Two zeolite samples were supplied by Société Méditerranéenne des Zéolithes (SOMEZ), including template-free powdered (0.5–1.0 μm) zeolite-X and powdered (<1.0 μm) natural chabazite. Initially, the zeolites were in the sodium form. However, in order to avoid Cd precipitation at the high pH of the Na-exchanged zeolites (NaX) and to mimic sorption processes in natural (calcium dominated) systems, the NaX was dialyzed against 0.1 M $Ca(NO_3)_2$ for 7–10 days at 25 °C to convert to the calcium form. The washing solution was replaced twice every day. Finally, samples were washed briefly with Milli-Q water, freeze-dried, and kept in closed polyethylene bottles. The chemical composition of Na- and Ca-exchanged zeolites was determined by XRF (Philips PW1400 X-Ray Fluorescence spectrometer, Department of Geology, University of Leicester). Major element analysis was performed on fused borate beads to eliminate mineralogical effects and to reduce inter-element effects. Fused bead analyses were re-calculated to incorporate the loss on ignition (LOI).

2.2. Methods

2.2.1. Determination of average particle size

The particle size distributions of CaX and CaCHA were determined by a laser diffraction technique using a Beckman Coulter LS230 laser particle analyzer which uses the polarization intensity differential scattering (PIDS) method and has a dynamic range between 0.04 and 2000 μm. Zeolites samples were prepared by dispersing ~1.0 g of solid in ~200 mL distilled water with a few drops of the surfactant Triton X-100 added. Because particle agglomeration cannot be avoided completely, the mean particle size of zeolite samples was determined by image analysis of SEM micrographs using an image-processing program, UTHSCSA Image Tool version 3.0 (Wilcox et al., 1996) and compared to that obtained from the diffraction method.

2.2.2. Preparation of zeolite suspensions

Stock suspensions of the calcium-exchanged zeolite-X (CaX) and chabazite (CaCHA) were equilibrated in 0.01 M $CaCl_2$ for 2 weeks, maintained at constant temperature (25 ± 2 °C) and equilibrated with air. The pH of the equilibrated suspensions of CaX and CaCHA were 7.30 ± 0.02 and 6.88 ± 0.02, respectively. All solutions were prepared with high purity water (~18 MΩ cm^{-1}) from a Millipore Milli-Q water purification system; all chemicals used in this investigation were of ACS or GR analytical grade.

2.2.3. Effect of Cd-speciation on sorption

Batch sorption experiments of Cd on CaX were conducted in 40 mL polycarbonate centrifuge tubes and at a solid: solution ratio (φ) of 1:55 with three replicates. Prior to addition of Cd, as $Cd(NO_3)_2$, suspensions were allowed to equilibrate with air for 2 weeks. Cadmium was added to the zeolite suspensions as a ^{109}Cd-spiked solution (~5.4 kBq μmol^{-1} in 0.01 M $CaCl_2$) to give Cd loadings of 9–132 mmol Cd kg^{-1} in three background electrolytes: $CaCl_2$, $Ca(NO_3)_2$, and a 1:1 mixture of $CaCl_2$ and $Ca(NO_3)_2$, all at ionic strengths of 0.03 M. Samples were gently mixed on a vertical rotary shaker (~10 rpm min^{-1}) and left to equilibrate for 5 and 25 days in a dark room at constant temperature (25 ± 2 °C). To measure the concentration of total dissolved Cd, at each contact time, supernatant samples were separated by centrifugation at 2200*g* for 30 min and filtration (<0.2 μm polyethersulfone (PES) membrane filter; Minisart®, Sartorius). Solutions were then weighed in counting vials for radio-assay of ^{109}Cd using a gamma-spectrometer with a 3 × 3 inch NaI detector system (Packard, COBRA-II). Blanks and standards were counted at the same time; all volumes in the counting vials were equal (4.0 mL) to ensure identical sample geometry.

Because ^{109}Cd was introduced to the solid phase premixed with stable Cd, the concentration of total sorbed Cd (Cd_{TS}, μmol Cd kg^{-1}) can be calculated as

$$Cd_{TS} = \frac{Cd_{Tot} - \left(\frac{A_{Soln(1)} \times V_{Soln}}{A^*}\right)}{W} \quad (1)$$

where Cd_{Tot} is the total amount of Cd added to the system (μmol), $A_{Soln(1)}$ is the radioactivity measured in the separated supernatant (Bq L^{-1}), V_{Soln} is the volume of solution (L), A^* is the specific activity of the Cd stock solution (Bq μmol^{-1} Cd), and W is the weight of zeolite (kg) in the suspension. The total Cd concentration in solution (Cd_{Soln}, μmol Cd L^{-1}) was calculated from Eq. (2)

$$Cd_{Soln} = \frac{A_{Soln(1)}}{A^*} \quad (2)$$

Chemical analysis (Flame-AES) was undertaken to measure the concentration of total dissolved Na, Ca, and K. The pH of the solution was measured routinely at the beginning and at the end of each contact time. All chemical and radiochemical analyses were conducted on three replicate samples. Cadmium in solution was speciated using the WHAM VI speciation model (Natural Environment Research Council (NERC), Windermere, UK) (Tipping, 1994; Lofts and Tipping, 1998; Tipping, 1998) to determine the free Cd ion activity, $\{Cd^{2+}\}$.

2.2.4. Determination of isotopically exchangeable Cd

To measure the concentration of isotopically exchangeable Cd, a 'double labeling' technique was applied. This involved the introduction of a second spike (0.2 mL) of carrier-free ^{109}Cd (~14 kBq mL^{-1} in 0.01 M $CaCl_2$) to equilibrated suspensions directly after the measurement of Cd_{Soln} by radio-assay of the first spike (Eq. (2)). Following a further isotope-equilibration time of 48 h (Young et al., 2000; Degryse et al., 2004), the solution phase was separated for a second radio-assay. The radioactivity in solution at that point, $A_{Soln(1+2)}$ (Bq L^{-1}), originates from both the first spike and the second spike of ^{109}Cd. Thus, the radioactivity in solution from the second spike of ^{109}Cd, $A_{Soln(2)}$ (Bq L^{-1}), can be calculated as:

$$A_{Soln(2)} = A_{Soln(1+2)} - A_{Soln(1)} \quad (3)$$

It was assumed that, during this second period of isotope-equilibration, ^{109}Cd from the second spike only mixed with the labile pool of Cd and did not access the non-labile sorption sites. The concentration of Cd in solution following equilibration of the second spike was estimated from a polynomial fit to the trend in Cd_{Soln} with time. In practice, this gave values ($Cd_{Soln(2)}$) which were almost identical to those measured after the first period of equilibration, 48 h earlier.

The amount of radioactivity from the second spike of ^{109}Cd transferred to the solid phase, A_{Solid} (Bq kg^{-1}), was calculated as

$$A_{Solid} = \frac{A_{Std2} - (A_{Soln(2)} \times V_{Soln})}{W} \quad (4)$$

where A_{Std2} (Bq) is the total radioactivity in the second spike of ^{109}Cd.

The assumptions behind this approach were tested by equilibrating Cd-spiked CaX samples for 40 days and measuring the concentration of isotopically exchangeable Cd after three different isotope-equilibration times for the second spike: 48, 72, and 120 h.

From Eqs. (3) and (4), the concentration of labile sorbed Cd (Cd_{LS}; μmol Cd kg^{-1}) can be determined as

$$Cd_{LS} = \frac{A_{Solid} \times Cd_{Soln(2)}}{A_{Soln(2)}} \quad (5)$$

It follows that non-labile Cd, Cd_{NL}, can be calculated from Eq. (1) as

$$Cd_{NL} = Cd_{TS} - Cd_{LS} \quad (6)$$

Labile sorbed Cd (Cd_{LS}) was determined in CaCHA samples once at the end of the experiment (40 d) whereas it was determined in CaX samples at each contact time (10, 20, 40, 60, and 100 d).

The effects of time on Cd sorption by CaX and CaCHA were studied using a batch technique similar to the method described earlier in Section 2.2.3. Sorption and desorption experiments were carried out at a range of added Cd concentrations 4.5–12 mmol Cd kg^{-1} ($\varphi = 1{:}75$), and 0.65–9.5 mmol Cd kg^{-1} ($\varphi = 1{:}60$) for CaX and CaCHA, respectively.

All sorption experiments were designed, following preliminary trials, with Cd loadings, φ, and contact times to produce solution Cd concentrations in the range of 0.05–30 μmol L^{-1} to be broadly comparable to previously measured soil pore water Cd concentrations presented in the literature—e.g., Tye et al. (2003) reported values of Cd_{Soln} for contaminated soils of 0.01- 32 μmol Cd L^{-1}.

2.2.5. Desorption of Cd from CaX

Following adsorption for a prescribed time, desorption was initiated by replacing ~50% of the supernatant solution with Cd-free desorbing solution and allowing samples to re-equilibrate (with shaking) over a period of 48 h. Supernatant samples were then separated for radio-assay as described before. This desorption procedure was repeated five times. With the small solid: solution ratio used in sorption/desorption experiments, the use of fresh electrolyte solution as a desorbing solution is not recommended in desorption studies. There are two reasons for this: (i) successive desorption events may change the pH of an equilibrated zeolite suspension and (ii) at each desorption step the established equilibrium with structural components of the solid (Si, Al), is disturbed; both factors may affect surface Cd sorption. To avoid these problems, a desorbing solution was prepared by equilibrating aerated suspensions of CaX in 0.01 M $CaCl_2$ at 25 ± 2 °C for 2 weeks prior to the desorption experiment. The supernatant solution of this suspension was used as the desorbing solution after being filtered (<0.2 μm PES filter) prior to use. The pH of the filtered desorbing solution was very close to that of the zeolite sample suspensions, and hence pH adjustments were

not necessary. This step ensures that virtually no changes in chemical speciation or pH occurred during desorption, other than the Cd concentration in solution.

2.3. Model development and modeling procedures

Is time-dependant Cd sorption by CaX controlled by reaction kinetics or diffusion into zeolite particles? To answer this question, Cd sorption was modeled using a first-order reaction kinetic model (KM model) and an intracrystalline diffusion model (DM model) that are described in Sections 2.3.1 and 2.3.2, respectively.

2.3.1. Formulation of the KM model

A deterministic model was developed to describe the sorption and subsequent immobilization of Cd^{2+} within CaX. The reactivity of sorbed Cd is defined in terms of two states, designated labile and non-labile. Labile sorbed Cd (Cd_{LS}) is assumed to be in constant dynamic equilibrium with the free ion activity of Cd^{2+}, $\{Cd^{2+}\}$, in solution, whereas non-labile Cd (Cd_{NL}) is assumed to be connected by a kinetically controlled process. A schematic representation of the model is shown in Fig. 1.

Instantaneous partitioning between Cd_{LS} and Cd^{2+} is assumed to be governed by a simple Freundlich isotherm

$$Cd_{LS} = k_F\{Cd^{2+}\}^n \tag{7}$$

From speciation analysis, the ratio (termed θ) of the concentration of total dissolved Cd to the free ion activity of Cd^{2+} can be obtained. Hence $\{Cd^{2+}\}$, μmol L^{-1}, can be calculated from the mass balance of the total labile Cd (Cd_{TL}, μmol Cd kg^{-1}) and combined with Eq. (7) to give

$$\{Cd^{2+}\} = [Cd_{TL} - (k_F\{Cd^{2+}\}^n)] \times \left(\frac{W}{V_{Soln} \times \theta}\right) \tag{8}$$

where Cd_{LS} is the labile sorbed Cd, μmol Cd kg^{-1}, Cd_{TL} is the total labile Cd, μmol Cd kg^{-1}, and the constants k_F and n are sorption coefficients.

Transfer between Cd_{LS} and Cd_{NL} (Fig. 1) were assumed to follow first-order kinetics.

Thus,

$$\frac{d(Cd_{TL})}{dt} = \frac{d(Cd_{NL})}{dt} = -k_1 Cd_{LS} + k_2 Cd_{NL} \tag{9}$$

The solution of Eq. (9) requires the following initial conditions:

$$[Cd_{TL}]_{t=0} = \frac{Cd_i \times V_{Soln}}{W} \tag{10}$$

and

$$[Cd_{NL}]_{t=0} = 0 \tag{11}$$

where k_1 and k_2 are rate coefficients (d^{-1}) whose values are estimated by fitting to experimental data and Cd_i is the concentration of added Cd (μmol L^{-1}).

2.3.1.1. Effect of initial Cd concentration on the values of adjustable parameters. Model KM assumes that the initial Cd concentration has no effect on the value of the adjustable parameters. However, the wide range of Cd concentrations used to construct the sorption isotherms raises the question of whether the approach to equilibrium is concentration-dependent. To address this question, a 'compound model' was developed that combined five KM sub-models, each describing a single Cd loading. For the range of Cd concentrations employed, we assumed that the initial Cd concentration will influence only the value of the parameter k_F in Eq. (7). Thus, each sub-model was assigned a different value for k_F and the other parameters k_1, k_2, and n were used globally in the compound model. The fitting procedure was undertaken as described earlier. To compare between the overall and the compound models, the minimum description length (MDL) method was used. MDL is a measure of generalizability that takes account of the possibility of overfitting. It is sensitive to the functional form of the model as well as to the number of parameters (Grunwald, 2000; Pitt and Myung, 2002; Myung and Pitt, 2004; de Brauwere et al., 2005). The model with the lowest MDL value is regarded as most suitable for purposes of predictions.

2.3.2. Formulation of the DM model

Because the zeolite suspension was agitated, both *bulk* and *film* diffusion can be neglected and the rate-limiting processes would be *intracrystalline* diffusion only. Assuming Fickian diffusion, for an isothermal system in which intracrystalline diffusion is the rate-controlling process

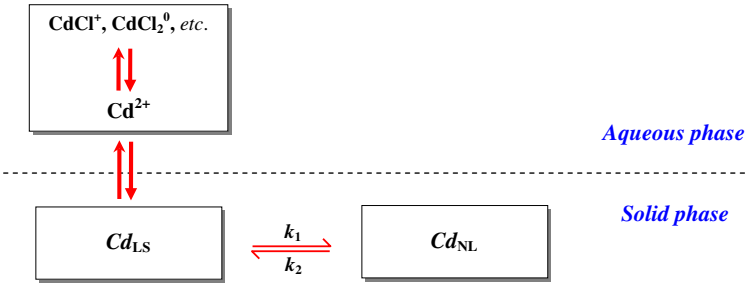

Fig. 1. Compartmental representation of the kinetic model of Cd sorption on zeolite-X. The arrows ⇄ represent dynamic equilibrium between components in the system whereas the arrows ⇌ denote kinetically controlled mass transfer; k_1 and k_2 are the rate coefficients describing transfer between labile and non-labile states.

the general diffusion equation for non-steady state in one direction is

$$\frac{\delta Cd_{NL}}{\delta t} = D\frac{\partial^2 Cd_{NL}}{\partial x^2} \quad (12)$$

where D is the apparent diffusion coefficient ($cm^2\ s^{-1}$).

Analytical solutions for the above transient diffusion equation have been obtained by integrating Eq. (12) between suitable boundary conditions for a given particle geometry and are widely used in the soil literature (Barrer, 1941; Crank, 1975; Kärger and Ruthven, 1992). Probably the most commonly used analytical solution is the one, which represents the case of a constant surface concentration. However, in our case, the surface concentration of Cd declines with time. Therefore, we have solved the differential equation (Eq. (12)) numerically in spherical geometry with a 'concentric shells diffusion model' which assumes that initially all labile Cd is present at the outer shell and with time Cd^{2+} diffuses through N concentric shells (e.g., 100 shells). Thus, the concentration of non-labile Cd is the sum of Cd^{2+} in all the internal shells.

2.3.3. Model implementation and parameter estimation

The models described were implemented using software within which the differential equations were solved by a fourth-order Runge–Kutta procedure. The bisection method was used to find the root of the implicit function in Eq. (8). This iterative method required two initial guesses to bracket both sides of the root. For both the kinetic (KM) and diffusion (DM) models, estimation of the adjustable parameters (k_F, n, k_1, k_2, D) was carried out using a Levenberg–Marquardt procedure, which minimizes the residual standard deviation (RSD)

$$RSD = \sqrt{\frac{\sum_{i=1}^{i=j}(O_i - P_i)^2}{df}} \quad (13)$$

where O_i and P_i are the log-transformed observed and predicted data, respectively, and df is the degree of freedom. All these methods are described in detail by Press et al. (2002).

3. Results and discussion

3.1. Chemical composition of zeolites

Data from XRF analysis for the as-received zeolites and the treated zeolites are reported in Table 1. The chemical compositions reported were converted from the weight percentage of the oxides. Data shows that ~69% and 92% Ca-exchange was achieved in chabazite and zeolite-X, respectively.

3.2. Particle size distribution (PSD)

Results obtained for the PSD using laser diffraction showed that the average radii (assuming spherical particles) of CaX and CaCHA were 1.25 and 23.2 μm, respectively. From analysis of SEM micrographs of zeolites, the mean particle radii of CaCHA were broadly similar to the laser diffraction values at 0.6 and 20.0 μm, respectively. Results from SEM micrographs are probably more reliable than laser diffraction especially when analyzing very small particles that have a tendency to agglomerate such as CaX. Therefore, the mean particle radii obtained from the analysis of SEM micrographs were used in the subsequent calculations.

3.3. Effect of Cd-speciation on Cd sorption

3.3.1. Effect of background electrolyte

A traditional presentation of a Cd sorption isotherm (i.e., Cd_{TS} against Cd_{Soln}), on CaX suggests that Cd sorption is affected by the composition of the background electrolyte and contact time (Fig. 2). To test whether Cd^{2+} alone controls the equilibrium with the solid phase and whether precipitation was likely, a speciation analysis using WHAM VI was undertaken. Initially, a systematic decrease in pH (up to 0.45 pH units) was observed with increasing concentration of added Cd (9–132 mmol Cd kg^{-1}). Saturation indices of $CaCO_3$(s) and $CdCO_3$(s) were less than unity, indicating that no precipitation should have occurred. Fig. 3 shows adsorption isotherms expressed as a function of the free ion activity $\{Cd^{2+}\}$, in $CaCl_2$, $Ca(NO_3)_2$, and $CaCl_2/Ca(NO_3)_2$ solutions. A single consistent trend is apparent, suggesting that the solid $\rightleftharpoons$ solution equilibrium is with Cd^{2+} alone. The charged Cd-complexes in 0.01 M $CaCl_2$ at the pH range 6.0–7.5 are dominated by Cd^{2+} and $CdCl^+$ whereas Cd^{2+} alone predominates in the $Ca(NO_3)_2$ medium. The hydrated species $[Cd(H_2O)_6]^{2+}$ and $[CdCl(H_2O)_5]^+$ possess octahedral symmetry and the bond distances Cd–O (2.32 and 2.34 Å , respectively) and Cd–Cl (2.5 Å) are very similar (Butterworth et al., 1992). Therefore, the slight difference in ion radius should not preclude sorption of $CdCl^+$ as both ions would be able to dif-

Table 1
Chemical compositions of the unit cell, pH, and theoretical CEC of chabazite and X-zeolite

Material	Chemical composition	pH[a]	Theoretical CEC[b] $cmol_c\ kg^{-1}$
NaCHA	$\lvert Ca_{0.1}Mg_{0.2}K_{0.2}Na_{2.1}\rvert [Al_{2.9}Si_{9.\ 0}O_{24}]$-CHA	6.92	372
CaCHA	$\lvert Ca_{1.1}Mg_{0.1}K_{0.1}Na_{0.4}\rvert [Al_{2.9}Si_{9.0}O_{24}]$-CHA	6.88	364
NaX	$\lvert Na_{84}\rvert [Al_{84}Si_{108}O_{384}]$-FAU	10.40	628
CaX	$\lvert Na_6Ca_{39}\rvert [Al_{84}Si_{108}O_{384}]$-FAU	7.42	639

[a] Measured in zeolites suspension in 0.01 M $CaCl_2$.
[b] Calculated from the anhydrous zeolite formula.

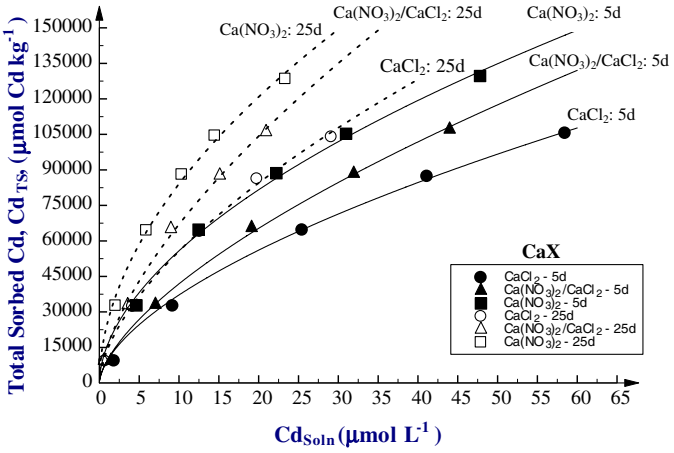

Fig. 2. Cd sorption, as a function of Cd_{Soln}, on CaX in three background electrolytes all at $I = 0.03$ M and at contact times of 5 and 25 days. Solid (5 d) and dotted (25 d) lines represent Freundlich isotherms fitted to observed data. Experimental error (as coefficient of variation) in Cd_{Soln} were less than 3%.

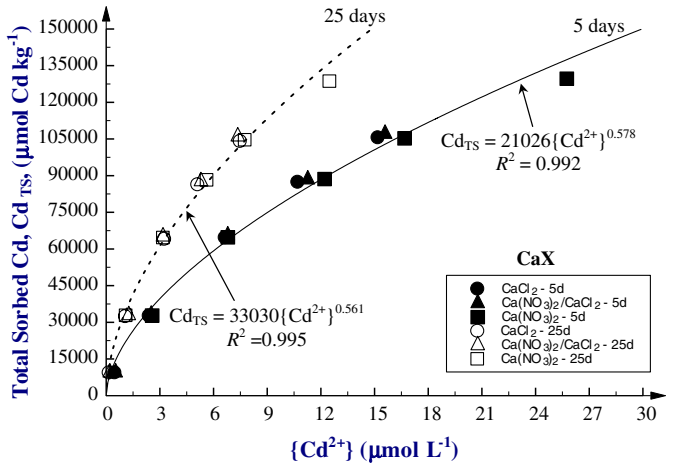

Fig. 3. Cd sorption, as a function of {Cd^{2+}}, on CaX in three background electrolytes all at $I = 0.03$ M and at contact times of 5 and 25 days. Solid (5 d) and dotted (25 d) lines represent Freundlich isotherms, Eq. (7), fitted to observed data.

fuse through the large cavities in CaX. However, the Si/Al ratio in CaX is ~1.3, which indicates a high charge density inside its cavities. According to Eisenman's model (Eisenman, 1962), zeolites with low Si/Al ratio have a highly negatively charged electrostatic field that gives good selectivity for divalent cations especially those with high hydration energy. Therefore, it might be concluded that the divalent cation Cd^{2+} ($\Delta H_{hyd} = -1806$ kJ mol^{-1}) will be preferred for sorption over the monovalent cation $CdCl^+$ ($\Delta H_{hyd} \approx -700$ kJ mol^{-1}; (Butterworth et al., 1992)); in fact adsorption of the latter appears to be negligible under the conditions used.

The electrolyte 0.01 M $CaCl_2$ was used in all subsequent sorption/desorption experiments so that the total concentration of Cd in solution was large enough to provide sufficient accuracy in the radio-assay of ^{109}Cd, while still maintaining low Cd^{2+} activity values. Note that although results shown in Figs. 2 and 3 have also been demonstrated for soils in previous studies, it was vitally important to show that Cd^{2+} dominates the solid: solution equilibrium for zeolites because, unlike whole soils, it was possible that monovalent forms of Cd (e.g., $CdCl^+$) could have been preferentially sorbed in specific locations in the zeolite structure. Fig. 3 also shows that the effect of time on Cd^{2+} sorption is marked, especially in relation to the Freundlich constant k_F, rather than the power term n. This is discussed in more detail in Section 3.5.

3.3.2. Effect of possible hydrolysis reactions

Based on the XRF analysis provided following Ca ion exchange of CaX (Table 1), the calculated CEC of the as-received NaX and CaX are very close if it is assumed that Ca is present solely as a divalent cation. Thus, there is no evidence of the formation of $CaOH^+$ as a sorbed cation due to zeolite hydrolysis reactions.

Partial hydrolysis of Cd could result in sorbed hydrolyzed species (i.e., $CdOH^+$, $Cd(OH)_2^0$, etc.); the formation of polymeric or multinuclear Cd-species such as $[Cd(H_2O)_{n\text{-}1}Cl]^+$ (Constable, 1984) is also possible. To the best of our knowledge, the formation of Cd clusters or polynuclear species within the small cavities of CaX at low Cd loadings, ambient temperature, and atmospheric pressure has not been reported. In addition, results from the WHAM speciation model suggested that Cd^{2+} and monomeric chloride complexes comprised approximately 99% of Cd in solution in the zeolite suspensions used in this study. Therefore, it seems reasonable to conclude that Cd^{2+} is the only sorbing species.

3.4. Testing the validity of the radio-labile assay

The radio-labile assay used here is valid provided ^{109}Cd from the second spike mixes only with a discrete 'labile' form of Cd. Fig. 4 shows that measuring the concentration of isotopically exchangeable Cd after isotope-equilibration times of 48, 72, or 120 h gives similar levels of labile Cd. This suggests that the use of an equilibration time of 48–72 h is satisfactory for complete mixing of ^{109}Cd with the labile Cd and that ^{109}Cd from the second spike does not access non-labile sorption sites. Hence, the application of the radio-labile assay to CaX appears to correctly describe a distinct 'pool' of chemically reactive Cd (i.e., provides a clear distinction between labile and non-labile Cd forms). Data for an isotope-equilibration time of 120 h appeared slightly displaced but this did not seem to arise from fixation of ^{109}Cd from the second spike because the 'apparent' labile Cd appeared to be slightly reduced.

3.5. Effect of time on Cd sorption by CaCHA over 40 days

The effect of time on Cd sorption by CaCHA was investigated; results are presented in Fig. 5. Sorption of Cd at different contact times was well described by a single Fre-

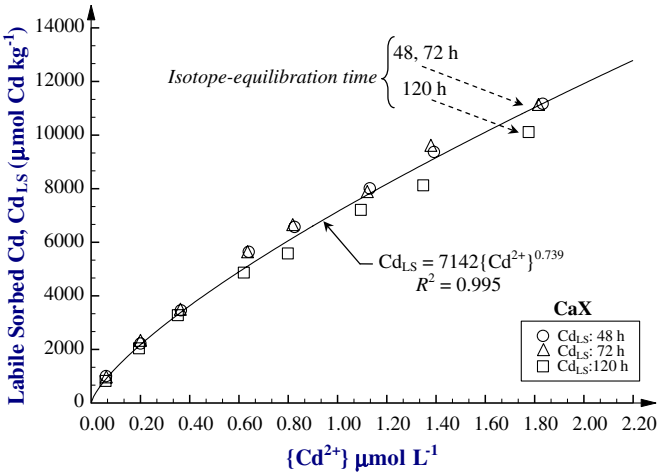

Fig. 4. Effect of isotope (^{109}Cd) equilibration time for 48, 72, and 120 h on the concentration of labile sorbed Cd as a function of {Cd^{2+}}. Measurements conducted after 40 d reaction time of Cd with CaX (in 0.01 M $CaCl_2$) using a double labeling technique. Experimental error (as coefficient of variation) in Cd_{Soln} were less than 5%.

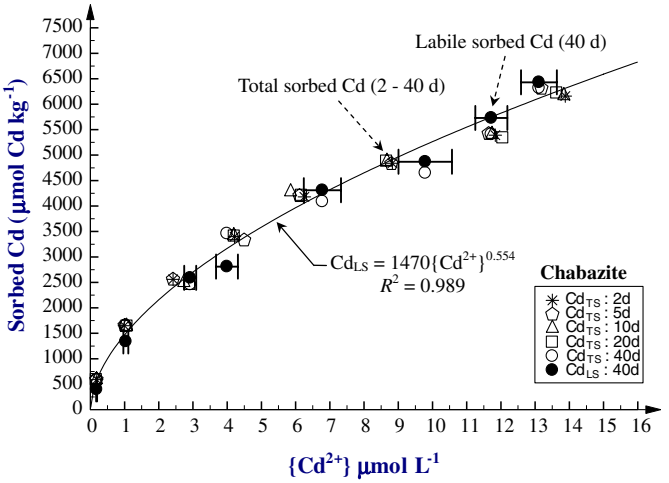

Fig. 5. Effect of contact time on Cd sorption by CaCHA as a function of {Cd^{2+}}. The symbols (○, □, △, ⬠, and ∗) are the total sorbed Cd at contact times of 2, 5, 10, 20, and 40 d, respectively, while the closed symbol (●) represents labile sorbed Cd at 40 d. The solid line represents a Freundlich isotherm fitted to all data. Experimental error (as coefficient of variation) in Cd_{Soln} was less than 8%, error bars are shown only for Cd_{LS} only, for clarity.

undlich isotherm. In addition, labile sorbed Cd closely followed the same sorption isotherm. Both results suggest that CaCHA acts as a perfect ion exchanger with no apparent fixation mechanism for Cd. This also suggests that the double labeling technique for measuring radio-labile Cd works satisfactorily.

3.6. Kinetics of Cd sorption by CaX

3.6.1. Effect of time on Cd^{2+} sorption by CaX over 100 days

Figs. 6 and 7 show a progressive increase in Cd sorption by CaX over time (10–100 days) and marked desorption hysteresis, respectively. In contrast, the relationship between Cd_{LS} and {Cd^{2+}} is remarkably constant and all labile Cd data can be *collectively* described by a single Freundlich relationship ($k_F = 12.1 \pm 0.290 \times 10^3$ L kg^{-1} and $n = 1.02 \pm 0.013$). The solid lines in Figs. 6 and 7 represent the fit of the kinetic model (KM, overall model) simultaneously to all the sorption and desorption data; i.e., model parameters (k_F, k_1, and k_2; Eqs. (7) and (9)) were parameterized using all data (Cd_{NL}, Cd_{LS}, {Cd^{2+}}, and Cd_{TS}) shown in Figs. 6 and 7 as a single set.

3.6.2. Analysis of the kinetic model

3.6.2.1. Model fitting. The KM model provides a good description of Cd^{2+} sorption, desorption, and fixation by CaX. The model shows a good fit ($R^2 = 0.999$; p-value < 0.001) to experimental data for Cd at different Cd loadings. To test the reliability of the model fitting, the initial estimates of the fitted parameters were varied widely prior to optimization and the results were similar.

The fitted values of the apparent rate coefficients k_1 and k_2 were $(42.0 \pm 0.61) \times 10^{-3}$ and $(9.00 \pm 0.22) \times 10^{-3}$ d^{-1}, respectively, indicating that the final equilibrium position favors Cd transport to the non-labile sites. The distribution of Cd (as %Cd) between the solution phase and labile and non-labile sites in the solid phase is presented in Fig. 8. After 100 d only 20% of Cd was labile while the remaining 80% was non-labile; after ~80 d Cd_{NL} approached an asymptote. Although the two-pool model presented in Fig. 1 may be a simplification, the shallow slope of the Cd_{NL} curve after ~80 d in Fig. 8 suggests that the introduction of further metal pools to the model described in Fig. 1 would require very precise data to be collected over a very long contact time for effective model parameterization. Thus, the two-pool model described in this study appears adequate for describing Cd sorption and desorption by CaX.

It is also possible that Cd is transferred to a non-labile form directly from the solution phase, rather than following initial sorption to labile sites, as we have assumed. Unfortunately, it is not possible to differentiate between these two possible pathways with the current data alone and so we cannot unequivocally identify the fixation route. This arises because of the (instantaneous) linear relationship ($n \approx 1$) between Cd_{LS} and {Cd^{2+}} in Eq. (7) which confounds any attempt to discriminate between the two possible models on the basis of goodness of fit.

3.6.2.2. Effect of initial Cd concentration. The estimated value of the power term of Freundlich model, n, was close to unity (Fig. 6) which indicates that in this Cd concentration range the effect of initial Cd concentration on the values of model parameters is negligible. This was confirmed by fitting the compound version of the KM model to experimental data, which did not show a significant improvement in fit over the overall version of the model.

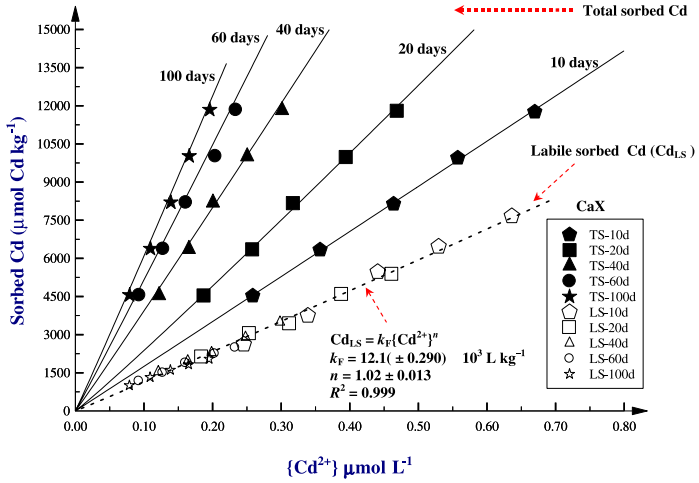

Fig. 6. Time-dependent Cd sorption on CaX as a function of $\{Cd^{2+}\}$. Solid lines represent the kinetic model KM (i.e., overall model) fitted to the total sorbed Cd data; the dotted line represents the same model fitted to the labile sorbed Cd data. Experimental error (as coefficient of variation) in Cd_{Soln} were less than 5%.

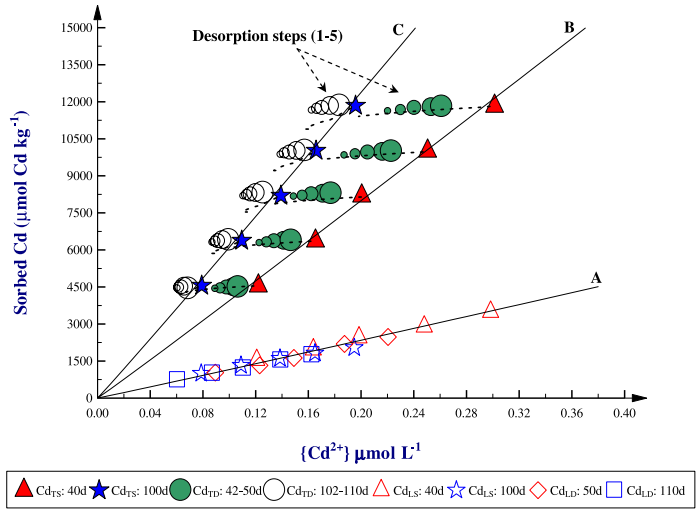

Fig. 7. Cd sorption and desorption isotherms on CaX following 40 d (▲) and 100 d (★) equilibration. Dotted lines represents the desorption trends as predicted from the kinetic model for five desorption steps. Closed (40 d) and open (100 d) circles represent the successive desorption steps following adsorption for 40 d and 100 d, respectively. Solid lines represent the kinetic model fit to the labile sorbed Cd at 40 and 100 days (solid line-A), total sorbed Cd at 40 d (solid line-B) and 100 d (solid line-C), respectively.

3.6.3. Desorption kinetics

As shown in Fig. 7, desorption of Cd^{2+} from CaX is characterized by an initial rapid release of Cd^{2+} ions, followed by a slower rate of Cd removal over longer contact times. If a 'zero-sink' situation was assumed (i.e., the reaction proceeds only with the backward reaction with $k_2 = 9.00 \times 10^{-3}$ d^{-1}) then the predicted half-time for Cd desorption was ~77 d. This suggests that if CaX was deployed as a permeable reactive barrier, or as a soil amendment, then the danger of Cd desorption in response to short-term reductions in solution concentration would be small.

3.6.4. Analysis of the diffusion model

It is well documented that the intracrystalline diffusion of ions is slower than ion diffusion in the solution phase (Helfferich, 1962). As shown in Table 2, the apparent diffusion coefficient (D), estimated from the DM model, is 2.84×10^{-19} cm^2 s^{-1} which is much smaller than the diffu-

Table 2
Comparison between the goodness of fit of the KM model and the DM model

	Diffusion model	Kinetic model[a]
R^2	0.969	0.987
RSD	0.0014	0.0005
MDL	13.13	14.17
$D \times 10^{-19}$ (cm^2 s^{-1})	2.84 ± 0.18	—

[a] Values of R^2, RSD, MDL were re-estimated by fitting the KM model to Cd_{NL} and Cd_{TL} data.

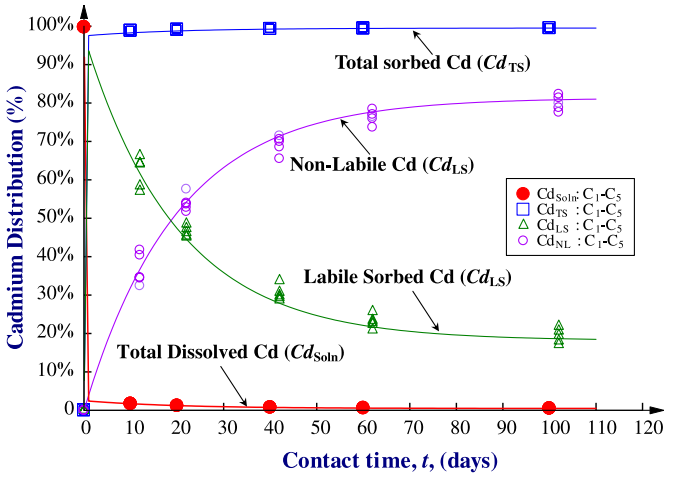

Fig. 8. Distribution of Cd (%) between different forms in CaX suspensions as a function of time. Fitted curves (solid lines) are model simulations (up to 100 d) for the sorption and fixation kinetics of Cd on CaX. Symbols (●, □, △, and ○) represents the experimental values of Cd_{Soln}, Cd_{TS}, Cd_{LS}, and Cd_{NL}, respectively, for the five Cd loadings (C_1–C_5) used in sorption experiments.

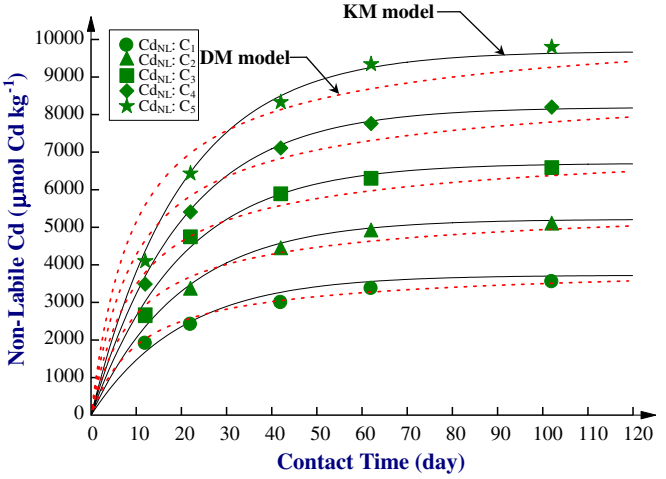

Fig. 9. Time-dependent Cd fixation by CaX using the KM model (solid lines) and the shell DM model (dotted lines). The symbols (●, ▲, ■, ★, and ◆) represents the experimental data at five increasing Cd concentrations (C_1–C_5) used in sorption experiments.

sion coefficient (D_I) of Cd^{2+} in solution, $D_I = 7.19 \times 10^{-6}\ cm^2\ s^{-1}$ (Horvath, 1985; Dobos, 1994).

A comparison of the DM model and the KM model performance required the re-estimation of R^2, RSD, and MDL for the KM model because the DM model considers Cd_{NL} and Cd_{TL} whereas the KM model was fitted using the Cd^{2+} and Cd_{LS} data (Table 2). Although, the MDL value of the DM model was slightly less than that of the KM model, the KM model shows better fitting ($R^2 = 0.987$) to observed data (see also Fig. 9) than the DM model ($R^2 = 0.969$). The use of a diffusion approach requires a number of constraining assumptions, which might result in fitting problems. To apply the diffusion model more mechanistically, the determination of the average particle size of sorbent, diffusion path, and tortuosity factor are all important. Unfortunately, experimental determination of these quantities is tedious, particularly the determination of diffusion path within zeolites that have three-dimensional channels such as faujasite and chabazite systems. Moreover, the final position in a diffusion model of this type is a homogeneous distribution of Cd within the sorbent. This means that at infinite time the surface concentration (i.e., Cd_{LS}) will approach zero. However, Fig. 8 showed that Cd_{LS} tends towards a non-zero asymptote at infinite time, constituting around 20% of sorbed Cd. Accordingly, we may conclude that diffusion models formulated with the underlying assumptions employed here are not suitable to model the process of Cd fixation in CaX system. It is possible to envisage an adapted form of the DM model in which, for example, the outer 20% of the particle volume is deemed to be instantly in equilibrium with the solution phase; the process of fixation then becomes diffusion into the inner 80%. However, dividing the solid into two hypothetical phases in this way produces a model, which is substantially similar to the kinetic (KM) model.

3.7. Linking sorption results to the framework structure of zeolites

3.7.1. Zeolite-X

Zeolite-X is a synthetic Al-rich counterpart of the natural mineral faujasite (FAU). It has a three-dimensional framework with sodalite cages (β-cages) viewed as the principal building blocks of the framework. The crystal structure of the faujasite system has been described by many authors and can be found elsewhere (Olson, 1970; Smith, 1976; Olson, 1995; Zhu and Seff, 1999). Exchangeable metal cations are usually distributed on specific sites of the zeolite-X framework. The principal sites are **I**, **I′**, **II**, **II′**, **III**, and **III′** whose positions are shown in Fig. 10. The number of extra-framework cations sorbed at each site differs according to the nature of the sorbed cation and whether the zeolite is hydrated or dehydrated. Ideally, site **I** can hold 16 monovalent cations per unit cell while the other sites can hold 32 each. However, cations simultaneously occupying sites **I** and **I′** share the face of a coordination polyhedron, which is not favored electrostatistically. This sharing problem is greater for sites **II** and **II′** (Smith, 1971). The diameter of free apertures of the α-cavity and the *S6R* in the faujasite system are ~7.4 and 2.2 Å, respectively (Breck, 1974). Because of its small hydration radius ~4.64 Å (Butterworth et al., 1992), $[Cd(H_2O)_6]^{2+}$ can diffuse easily through the α-cavity. However, these fully hydrated Cd^{2+} ions cannot diffuse into sodalite cavities or hexagonal prisms without losing some water of hydration. This dehydration step may represent an energy barrier to Cd^{2+} sorption and may therefore explain the time-dependant Cd^{2+} sorption on CaX.

Early studies of rapid ion exchange, showed that most Ca^{2+} ions in hydrated CaX occupy sites **I′** and **II′** whereas

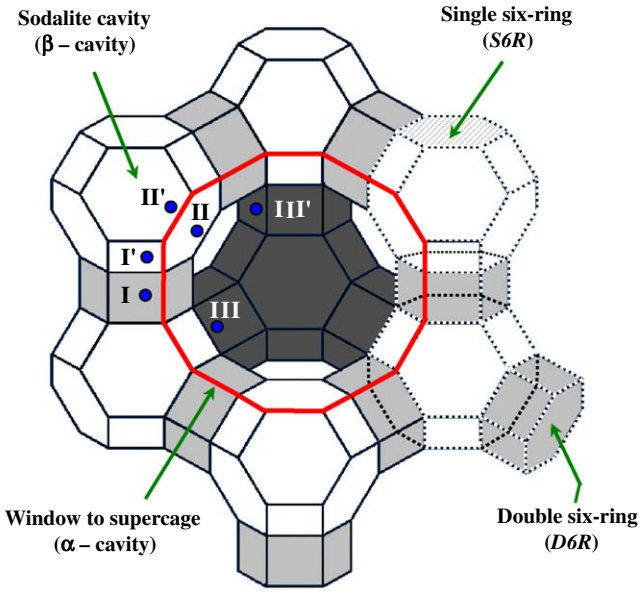

Fig. 10. A model of the faujasite (X- and Y-zeolite) unit cell, adapted from (Olson, 1970). Near the centre of each line segment is an oxygen atom. Si and Al atoms alternate at the tetrahedral intersections, except that Si substitutes for Al at about 4% of the Al positions. Exchangeable cations are found in site **I** at the centre of a *D6R*; site **II** at the centre of the *S6R*, or displaced from this point into a supercage; sites **I′** and **II′** lie in the sodalite cavity, on the opposite sides of the corresponding *S6R* from sites **I** and **II**, respectively; site **III** on a twofold axis opposite a 4-ring inside the supercage and site **III′** off site **III**. The eighth sodalite cavity was removed from this diagram for simplicity and it is orthogonal to the diagram.

site **III′** is partially occupied. Sites **I** and **III** are left empty of Ca^{2+} whereas site **II** is filled with H_2O (Breck, 1974). More recently, Calligaris et al. (1986) ion exchanged single NaX crystals at room temperature for 40 days and studied the distribution of Cd^{2+} in hydrated Cd-exchanged zeolite-X from refined X-Ray diffraction results. They found that site **I** was empty while site **I′** was nearly fully occupied by Cd^{2+} and, because site **II′** was fully occupied by H_2O, they suggested that each sodalite cavity was nearly completely filled by $[Cd(H_2O)]_4^{8+}$ clusters. Thus, in conclusion Calligaris et al. (1986) suggested that 29.8 out of 44 Cd^{2+} ions were located in small-pore regions of hydrated CaX. Unfortunately, in our study, determining the distribution of sorbed Cd^{2+} at various ion exchange sites was not possible. In order to work at environmentally relevant concentrations, the Cd loading on CaX was well below the saturation point of any of the recognized exchange sites (see Table 1). Furthermore, the fractionation of Cd^{2+} into labile and non-labile forms does not, in itself, reveal the location or hydration state of sorbed Cd within the zeolite structure. Nevertheless it seems reasonable to suggest that Cd^{2+} ions sorbed at the partially occupied sites **II**, **III**, and **III′** and probably at exchange sites on the external surface of the zeolite would be 'labile'. Equilibrium with these sites is expected to be rapid. A longer reaction time may be required for hydrated Cd^{2+} ions to enter sites **I′** and **II′** which can provide a favorable octahedral coordination position for Cd^{2+} ions. The energy barrier to sorption may be overcome if $[Cd(H_2O)_6]^{2+}$ loses part of its water of hydration and this may be the source of the time-dependant Cd^{2+} sorption by CaX and the desorption hysteresis observed. It is also possible that Cd^{2+} ions prefer to enter site **I** at low Cd loadings and subsequently undergo slow dehydration inside the *D6R* cages.

3.7.2. Chabazite

The framework of chabazite consists of *D6R* units arranged in layers and linked by 'twisted 4-rings' (Baerlocher et al., 2001). These *D6R* units have similar dimensions to those in the faujasite system. The resulting three-dimensional framework contains large ellipsoidal cavities with dimensions of 6.4×6.9 Å (for hydrated chabazite) but with a minimum aperture diameter of 3.8 Å (Smith, 1988; Baerlocher et al., 2001). The location of four cation exchange sites have been identified in hydrated Na-, Ca-, Sr-, and K-exchanged chabazite (Alberti et al., 1982). Only one site is located inside the *D6R* unit and the remaining three sites are located in the ellipsoidal cavity. The cation exchange capacity of chabazite is much lower than that of zeolite-X (Table 1). According to Eisenman's model (Eisenman, 1962), chabazite has an intermediate Si/Al ratio and therefore a preference for monovalent cations or divalent cations with low hydration energies. Therefore, Cd^{2+} replacement of existing cations within the small pores in chabazite may be less energetically favorable because of the high hydration energy of Cd^{2+} ($\Delta H_{hyd} = -1828$ kJ mol^{-1}; Dasent, 1982) and the high-energy barrier for diffusion to small pores. Consequently, sorbed Cd^{2+} would be expected to occupy the three cation exchange sites in the ellipsoidal cavity and non-specific sorption is therefore likely to be the dominant mechanism for Cd sorption in CaCHA. This would be consistent with the lack of any time-dependence to Cd sorption by CaCHA and with the observation that sorbed Cd remains isotopically exchangeable even after a prolonged contact time (Fig. 5).

4. Conclusion

This work has demonstrated time-dependent Cd sorption and desorption by CaX and how isotopic dilution can be used to quantifying transfer of sorbed Cd between labile and non-labile forms. It is speculated that Cd^{2+} ions may slowly access the sodalite cavity and possibly the *D6R* rings in CaX over time. The rate at which Cd accesses the small pores in CaX may be determined by the kinetics of Cd^{2+} ion dehydration. The 'fixation' of Cd in CaX is not irreversible but may be described as a 'slowly reversible' process. In contrast to CaX, CaCHA showed perfect ion exchange properties, even after prolonged contact times (up to 40 days). It is thought that this may be due to the small pore size of cages in CaCHA, which precludes any time-dependent sorption of Cd.

A reversible first-order kinetic model combined with a Freundlich sorption relation for labile Cd successfully described reversible sorption of Cd^{2+}, time-dependent fixation of sorbed Cd and desorption hysteresis with effectively just three fitted parameters. An intra-particle diffusion model provided a much poorer fit, both in terms of observed trend and final ratio of labile: non-labile Cd.

Acknowledgments

We thank AlTajir Trust for their generous financial support. We also thank Mr. W. Balmer at SOMEZ-France for supplying us with zeolite samples. Moreover, we thank Prof. J.R. Haas and the anonymous reviewers for their useful comments.

Associate editor: Johnson R. Haas

References

Alberti, A., Galli, E., Vezzalini, G., Passaglia, E., Zanazzi, P.F., 1982. Position of cations and water molecules in hydrated chabazite. Natural and Na-, Ca-, Sr-, and K-exchanged chabazites. *Zeolites* **2**, 303–309.

Baerlocher, Ch., Meier, W.M., Olson, D.H., 2001. *Atlas of Zeolite Framework Types*. Elsevier Scientific Publishing Co., Amsterdam.

Barrer, R.M., 1941. *Diffusion in and Through Solids*. Cambridge University Press, New York.

Barrer, R.M., Davies, J.A., Rees, L.V.C., 1969. Thermodynamics and thermochemistry of cation exchange in chabazite. *J. Inorg. Nucl. Chem.* **31**, 219.

Barrer, R.M., Rees, L.V.C., Bartholo, R.F., 1963. Ion exchange in porous crystals-1: self- and exchange-diffusion of ions in chabazites. *J. Phys. Chem. Solids* **24**, 51.

Barros, M.A.S.D., Silva, E.A., Arroyo, P.A., Tavares, C.R.G., Schneider, R.M., Suszek, M., Sousa-Aguiar, E.F., 2004. Removal of Cr(III) in the fixed bed column and batch reactors using as adsorbent zeolite NaX. *Chem. Eng. Sci.* **59**, 5959–5966.

Biskup, B., Subotic, B., 1998. Removal of heavy metal ions from solutions by means of zeolites. I. Thermodynamics of the exchange processes between cadmium ions from solution and sodium ions from zeolite A. *Sep. Sci. Technol.* **33**, 449–466.

Biskup, B., Subotic, B., 2000. Removal of heavy-metal ions from solutions by means of zeolites. II. Thermodynamics of the exchange processes between zinc and lead ions from solutions and sodium ions from zeolite A. *Sep. Sci. Technol.* **35**, 2311–2326.

Breck, D.W., 1974. *Zeolite Molecular Sieves: Structure, Chemistry, and Use*. John Wiley & Sons, Inc., New York.

Butterworth, P., Hillier, I.H., Burton, N.A., Vaughan, D.J., Guest, M.F., Tossell, J.A., 1992. Calculations of the structures, stabilities, Raman-spectra, and NMR-spectra of CdCln (OH2) a2-n, CdBrn (OH2) a2-n, and ZnCln (OH2) a2-n species in aqueous-solution. *J. Phys. Chem.* **96**, 6494–6500.

Calligaris, M., Nardin, G., Randaccio, L., Zangrando, E., 1986. Crystal structures of the hydrated and partially dehydrated forms of Cd-X exchangeable zeolites. *Zeolites* **6**, 439–444.

Colella, C., 1996. Ion exchange equilibrium in zeolite minerals. *Miner. Deposita* **31**, 554–562.

Constable, E.C., 1984. Zinc and cadmium. *Coord. Chem. Rev.* **58**, 1–51.

Crank, J., 1975. *The Mathematics of Diffusion*. Clarendon Press, Oxford.

Dasent, W.E., 1982. *Inorganic Energetics: An Introduction*. Cambridge University Press, Cambridge.

de Brauwere, A., de Ridder, F., Pintelon, R., Elskens, M., Schoukens, J., Baeyens, W., 2005. Model selection through a statistical analysis of the minimum of a weighted least squares cost function. *Chemometr. Intell. Lab.* **76**, 163–173.

Degryse, F., Buekers, J., Smolders, E., 2004. Radio-labile cadmium and zinc in soils as affected by pH and source of contamination. *Eur. J. Soil Sci.* **55**, 113–122.

Dobos, D., 1994. *A Handbook for Electrochemists in Industry and Universities*. Elsevier Scientific Publishing Co., Amsterdam, The Netherlands.

Dyer, A., 1988. *An Introduction to Zeolite Molecular Sieves*. John Wiley & Sons, Inc., Bath, UK.

Eisenman, G., 1962. Cation selective glass electrodes and their mode of operation. *Biophys. J.* **2**, 259–323.

Fletcher, P., Townsend, R.P., 1982. Transition metal ion exchange in mixed ammoniumsodium X and Y zeolites. *J. Chromatogr. A* **238**, 59–68.

Fletcher, P., Townsend, R.P., 1985. Ion exchange in zeolites: the exchange of cadmium and calcium in sodium X using different anionic backgrounds. *J. Chem. Soc. Faraday Trans. I* **81**, 1731–1744.

Garcia-Sosa, I., Solache-Rios, M., 2001. Cation-exchange capacities of zeolites A, X, Y, ZSM-5 and Mexican erionite compared with the retention of cobalt and cadmium. *J. Radioanal. Nucl. Chem.* **250**, 205–206.

Grunwald, P., 2000. Model selection based on minimum description length. *J. Math. Psychol.* **44**, 133–152.

Helfferich, F., 1962. *Ion Exchange*. McGraw-Hill, Inc., New York.

Horvath, A.L., 1985. *Handbook of Aqueous Electrolyte Solutions*. Ellis Horwood Ltd., West Sussex, UK.

Kärger, J., Ruthven, D.M., 1992. *Diffusion in Zeolites and Other Microporous Solids*. Wiley-Interscience, New York.

Keane, M.A., 1998. The removal of copper and nickel from aqueous solution using Y zeolite ion exchangers. *Colloids Surf. A* **138**, 11–20.

Kim, J.S., Keane, M.A., 2002. The removal of iron and cobalt from aqueous solutions by ion exchange with Na-Y zeolite: Batch, semi-batch and continuous operation. *J. Chem. Technol. Biotechnol.* **77**, 633–640.

Lai, P.P., Rees, L.V.C., 1976. Szilard-chalmers cation recoil studies in zeolites X and Y.1. Ion-exchange in zeolites X and Y. *J. Chem. Soc. Faraday Trans. I* **72**, 1809–1817.

Lofts, S., Tipping, E., 1998. An assemblage model for cation binding by natural particulate matter. *Geochim. Cosmochim. Acta* **62**, 2609–2625.

Myung, I.J., Pitt, M.A., 2004. In: *Methods in Enzymology*. Academic Press, pp. 351–366.

Nava, I., Garciasosa, I., Solacherios, M., 1995. Removal of Co and Cd by zeolite-X. *J. Radioanal. Nucl. Chem. Ar.* **191**, 83–87.

Nikashina, V.A., Zvereva, L.I., Olshanova, K.M., Potapova, M.A., 1976. Study of the selectivity of different types of zeolites towards some non-ferrous metals. *J. Chromatogr. A* **120**, 155–158.

Olson, D.H., 1970. A reinvestigation of crystal structure of zeolite hydrated NaX. *J. Phys. Chem.* **74**, 2758.

Olson, D.H., 1995. The crystal structure of dehydrated NaX. *Zeolites* **15**, 439–443.

Pitt, M.A., Myung, I.J., 2002. When a good fit can be bad. *Trends Cogn. Sci.* **6**, 421–425.

Press, W.H., Teukolsky, S.A., Vetterling, W.T., Flannery, B.P., 2002. *Numerical Recipes in C++: The Art of Scientific Computing*. Cambridge University Press, Cambridge, UK.

Shevade, S., Ford, R.G., 2004. Use of synthetic zeolites for arsenate removal from polluted water. *Water Res.* **38**, 3197–3204.

Smith, J.V., 1971. In: Gould, R.F. (Ed.), *Molecular Sieve zeolites-I*, chap. 15. American Chemical Society, pp. 171–200.

Smith, J.V., 1976. In: Rabo, J.A. (Ed.), *Zeolite Chemistry and Catalysis*, chap. 1. American Chemical Society, pp. 3–79.

Smith, J.V., 1988. Topochemistry of Zeolites and Related Materials.1. Topology and Geometry. *Chem. Rev.* **88**, 149–182.

Tipping, E., 1994. WHAM: A chemical-equilibrium model and computer code for waters, sediments, and soils incorporating a discrete site electrostatic model of ion-binding by humic substances. *Comput. Geosci.* **20**, 973–1023.

Tipping, E., 1998. Humic ion-binding model VI: An improved description of the interactions of protons and metal ions with humic substances. *Aquat. Geochem.* **4**, 3–48.

Tye, A.M., Young, S.D., Crout, N.M.J., Zhang, H., Preston, S., Barbosa-Jefferson, V.L., Davison, W., McGrath, S.P., Paton, G.I., Kilham, K., Resende, L., 2003. Predicting the activity of Cd^{2+} and Zn^{2+} in soil pore water from the radio-labile metal fraction. *Geochim. Cosmochim. Acta* **67**, 375–385.

Wilcox, D.C., Dove, B.S., McDavid, D.W., Geer, D.B. UTHSCSA ImageTool 3.0. 1996. San Antonio, Texas, USA, University of Texas Health Sciences Centre.

Young, S.D., Tye, A.M., Carstensen, A., Resende, L., Crout, N., 2000. Methods for determining labile cadmium and zinc in soil. *Eur. J. Soil Sci.* **51**, 129–136.

Zhu, L., Seff, K., 1999. Reinvestigation of the crystal structure of dehydrated sodium zeolite X. *J. Phys. Chem. B* **103**, 9512–9518.